Seventh International Conference

ECOLOGICAL ENGINEERING AND ENVIRONMENT PROTECTION (EEEP'2021)

with Youth Scientific Session and MELiSSA Summer University

30 September -3 October 2021, Varna, Bulgaria

MONITORING OF THE PHYSIOLOGICAL STATES OF FED-BATCH FERMENTATIONS WITH E.COLI

Anastasiya Zlatkova, Velislava Lyubenova

Institute of Robotics - BAS

INTRODUCTION

The fermentation processes with E.coli are known to go through several physiological states, which are described with different operating models. In this investigation a new key marker that recognizes the transition from one state into another is proposed - the dynamics of the intermediate metabolite acetate. In this study, a new marker was proposed to recognize the transition from one state to another and to switch from one model to another. Based on the derived operating models, the new key marker - the dynamics of the intermediate metabolite acetate and experimental data of two fed-batch fermentations with E.coli, two cascade structures of software sensors are developed. After analysis of the stability and adjustment of the software sensors (SS), the results of simulation studies at different disturbances are presented.

SOFTWARE SENSORS AND NEW MARKER

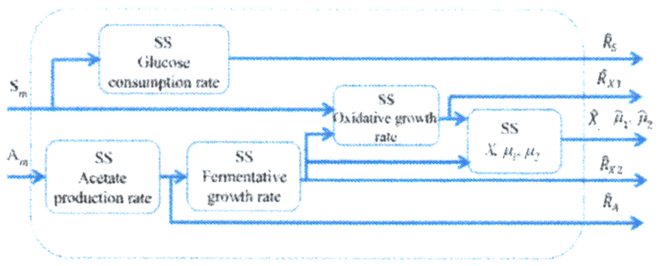

Fig. 1 Cascade structure of the software sensor for monitoring of two metabolic states

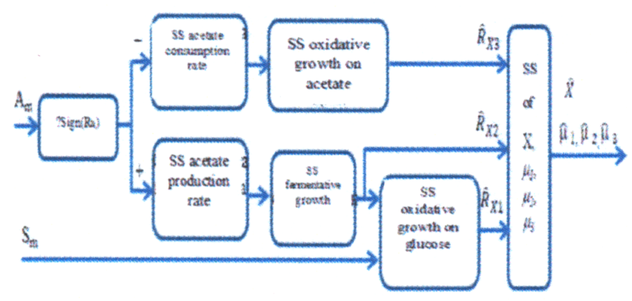

Fig. 2 Cascade structure of the software sensor for monitoring of three metabolic states

$$\frac{d}{dt}\begin{bmatrix} X \\ S \\ A \end{bmatrix} = \begin{bmatrix} 1 \\ -k_1 \\ 0 \end{bmatrix} \mu_1(t).X - D\begin{bmatrix} X \\ S \\ A \end{bmatrix} + \frac{F_{in,s}}{W}\begin{bmatrix} 0 \\ S_{in} \\ 0 \end{bmatrix}$$

$$\frac{d}{dt}\begin{bmatrix} X \\ S \\ A \end{bmatrix} = \begin{bmatrix} 1 & 1 \\ -k_1 & -k_2 \\ 0 & k_3 \end{bmatrix}\begin{bmatrix} \mu_1(t) \\ \mu_2(t) \end{bmatrix} X - D\begin{bmatrix} X \\ S \\ A \end{bmatrix} + \frac{F_{in,s}}{W}\begin{bmatrix} 0 \\ S_{in} \\ 0 \end{bmatrix} \quad (1)$$

$$\frac{d}{dt}\begin{bmatrix} X \\ S \\ A \end{bmatrix} = \begin{bmatrix} 1 & 1 \\ -k_1 & -k_2 \\ 0 & k_3 \end{bmatrix}\begin{bmatrix} \mu_1(t) \\ \mu_2(t) \end{bmatrix} X - D\begin{bmatrix} X \\ S \\ A \end{bmatrix} + \frac{F_{in,s}}{W}\begin{bmatrix} 0 \\ S_{in} \\ 0 \end{bmatrix} \quad (2)$$

$$\frac{d}{dt}\begin{bmatrix} X \\ S \\ A \end{bmatrix} = \begin{bmatrix} 1 & 1 \\ -k_1 & 0 \\ 0 & -k_4 \end{bmatrix}\begin{bmatrix} \mu_1(t) \\ \mu_3(t) \end{bmatrix} X - D\begin{bmatrix} X \\ S \\ A \end{bmatrix} + \frac{F_{in,s}}{W}\begin{bmatrix} 0 \\ S_{in} \\ 0 \end{bmatrix}$$

$$R_a = \frac{dA}{dt} + \frac{F_{in,S}}{W} A \quad (3)$$

Ra ≥ 0, S > 0	oxidative-fermentative growth on glucose
Ra < 0, S > 0	oxidative growth on glucose and acetate
Ra < 0, S = 0	oxidative growth on acetate

On figure 1 is shown the structure of the SS (SS1) derived on the basis of operating models (1) and the new key parameter the dynamics of acetate (3) for monitoring of two physiological states, which are oxidative and oxidative-fermentative growth on glucose. On figure 2 is the structure of the SS (SS2) based on model (2) and parameter (3) for monitoring of three physiological states, which includes all the metabolic states shown above. The input information for the two software sensors includes real-time measurements of acetate and glucose concentrations. Depending on the values of Ra, there are two cases for SS1 - for Ra equal to zero, the structure is reduced only to the third step of the cascade. For values greater than zero, the entire structure is activated. Similarly to SS1, the SS2 structure is activated depending on the values of Ra, and here the cases are 3, as shown above with the values indicating which of the three metabolic states the process is in.

RESULTS AND DICUSSION

Table 1. Parameter values of model 1

Parameter	$q_{s,max}$	K_s	k_1	k_2	k_3	k_{os}	q_{omax}	K_{io}
Value	2.044	0.148	2.67	20.59	10.77	2.184	0.685	20.198

Table 2. Parameter values of model 2

Parameter	$q_{s,max}$	K_s	k_1	k_2	k_3	k_4	k_{os}	q_{omax}	$K_{i,o}$	$q_{ac,max}$	K_a	K_{ia}
Value	11.34	7.17	2.06	3.17	0.72	8.9	5.47	0.28	2.8	0.04	0.37	84.8

An analysis of the simulation studies in the proposed SS is made, as the parameters of the models are presented in Tables 1 and 2. Figures 3, 4 and 5 show the simulation studies for SS1 both with added and not added white noise ε to the acetate (Fig. 4) and glucose (Fig. 5) measurements, whose average deviation represents 1% of the average value of their concentration. Two eigenvalues were tested: h = -25 and h = -12.5 whose choice is a compromise between the rate of convergence and the sensitivity of the estimates for the considered disturbances. Figure 3 estimates the oxidative and fermentative growth rates without disturbance. The larger relative errors are due to the lower values of the parameters during the jump at the beginning of the fermentative growth. The next two figures (4 and 5) show the estimates of the same rates, but with 3% noise in glucose measurements and 1% noise in acetate measurements. Estimation errors decrease within acceptable limits when higher eigenvalues are selected. The more inaccurate result in Figure 5 is explained by the low values of glucose concentration and the stronger influence of acetate noise.

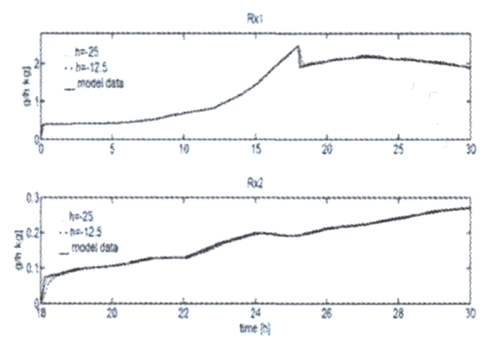

Fig. 3

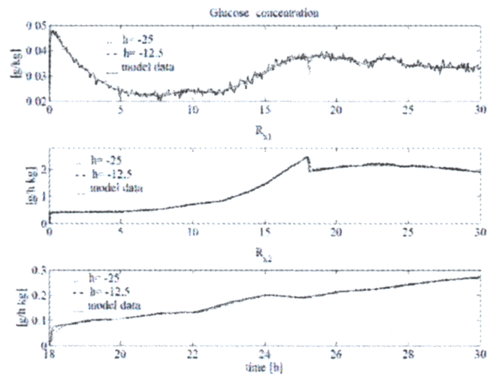

Fig. 4

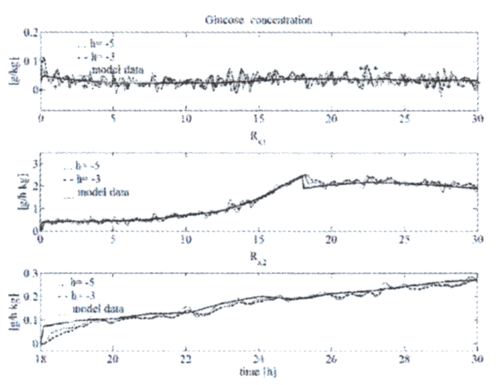

Fig. 5

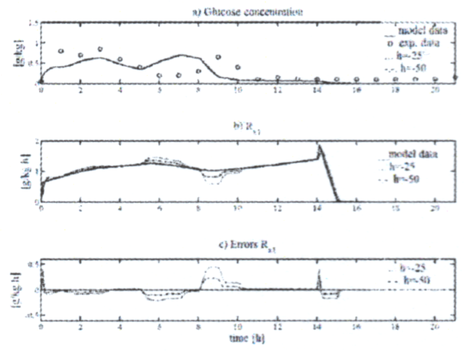

Fig. 6

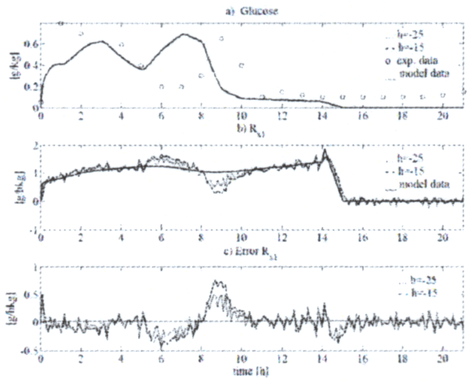

Fig. 7

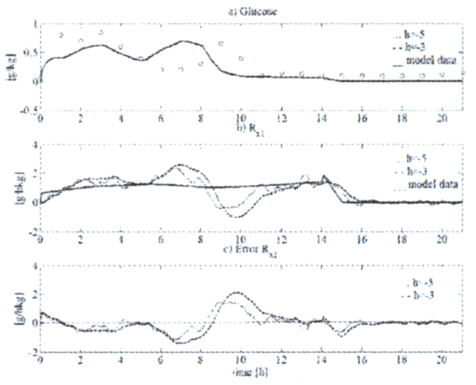

Fig. 8

Figures 6, 7 and 8 show the results of the simulation studies for SS2 similar to the previous ones. Figure 6 shows the results without disturbance in the measurements. The studies were realized at two eigenvalues -25 and -50. The estimation errors in *Rx2* affect the accuracy of *Rx1* ones. This can be seen from the errors between 5 and 10 hour in Figure 6b. The sharp changes in the estimates of *Rx1* are due to the fact that *Rx1* derivative is a disturbance at the beginning and end of the estimation. The maximum relative errors are 40% at h = -25 and 20% at h = -50. Figure 7 shows the results with 3% noise on the measurements of S. In this study, due to the strong influence of the high eigenvalue -50 on the sensitivity of the estimates, it was replaced by a lower -15. This reduces the effect of measurement noise, but also the accuracy and convergence of estimates under the influence of other disturbance, especially the *dRap / dt* derivative. Figure 8 shows the effect of the 1% noise included in the acetate measurements on the accuracy of the *Rx1* estimates. The use of lower eigenvalues is due to the stronger influence of noise in acetate on the accuracy of estimates compared to that for noise in glucose. The estimates have significant deviations, which shows that it is necessary for the measurement data to be previously filtered.

CONCLUSION

The quality of the evaluations is more strongly influenced by the noise when measuring acetate compared to that of glucose, which is due to the different levels of concentrations of these variables during fermentation. The setting of the proposed software sensors is reduced to the choice of a single eigenvalue, which is defined as a compromise between the rate of convergence of the estimates and their sensitivity to interference. Errors of the fermentative growth rate do not have a significant effect in Fermentation 1, while in Fermentation 2 this effect is significant. This can be explained by the different dynamics of these rates in the two fermentations. The effect of noise from glucose and acetate measurements is stronger in Fermentation 2 and also the errors in the estimation of the biomass concentration are higher in for that fermentation.

ACKOWLEDGEMENTS : This research has been supported by the National Scientific Fund of Bulgaria under the Grant КП-06-Н32/3 "Interactive System for Education in Modelling and Control of Bioprocesses (InSEMCoBio)"